



# Biosynthesis of Silver Nanoparticles from *Callistephus chinensis* Flower Waste: Evaluation of Antibacterial, Anticancer, and Contaminated Water Remediation Applications

Shruti Kakodkar\*, Pranjali Dhawal, Janvi Kadam, Rumanna Khan, Pradnya Shewale, and Tejaswi Chaukekar

Received : January 7, 2025

Revised : May 11, 2025

Accepted : June 8, 2025

Online : July 19, 2025

## Abstract

The present study explored antibacterial and anticancer properties of silver nanoparticles (AgNPs) uniquely synthesized using aster (*Callistephus chinensis*) flower waste (AFW) via a microwave-assisted approach. The nanoparticles were also tested for their effectiveness in treating coliform-contaminated borewell water. The AFW extract was characterized using LC-HRMS and quantitatively analysis using TPC and TFC assays. Nanoparticle characterization was performed using UV-spectroscopy, FT-IR, SEM, EDX, TEM, SAED and XRD instruments. The AFW extract showed 1.6687 mg of gallic acid equivalent (GAE) and 9.71 mg quercetin equivalent TPC and TFC, respectively. The LC-HRMS profile also revealed the presence of various polyphenols followed by organic acids and alkaloids. The minimum inhibitory concentration required to inhibit 90% of bacterial growth (MIC90) was determined against *Escherichia coli*, *Pseudomonas aeruginosa*, and *Staphylococcus aureus*. The cytotoxic activity of AgNPs was analyzed against cervical cancer cell line HeLa and normal human dermal fibroblast (HDF) cells. AgNPs exhibited a strong antibacterial activity, with MIC90 of 0.0625 mg/mL against *E. coli* and *P. aeruginosa*, and 0.125 mg/mL against *S. aureus*. Nanoparticle treatment did not alter the physicochemical parameters of borewell water beyond their permissible limits. According to MPN analysis, untreated borewell water contained 1600 coliforms/100 mL, which were eliminated following nanoparticle treatment (0 coliforms/100mL). AgNPs displayed anticancer activity against HeLa cell lines with an inhibitory concentration (IC<sub>50</sub>) of 0.21 mg/mL. The IC<sub>50</sub> of AgNPs against normal HDF cells was 0.414 mg/mL — higher than that observed against HeLa cell lines and the bacterial MIC90, thus indicating selective cytotoxicity. To conclude, the study demonstrated the promising use of AFW in the green synthesis of AgNPs, which exhibited potent antibacterial and anticancer properties, along with low toxicity to HDF cell lines. These AgNPs also demonstrated promising applications in treating coliform-contaminated borewell water.

**Keywords:** antibacterial, anticancer, flower waste, green synthesis, silver nanoparticles, water treatment

## 1. INTRODUCTION

The dynamic field of nanotechnology focuses on exploring the versatile applications of nanoparticles, which are highly dependent on their dimension, shape, and morphology. Given that the behavior of nanoparticles is strongly governed by their physical attributes, metal nanoparticles have become the focal point of numerous research studies due to their unique properties and applications [1]. Among the vast array of metal nanoparticles, silver nanoparticles (AgNPs) have garnered substantial interest because of their promising catalytic,

electronic, sensing, and medical applications [2][3].

Infectious diseases caused by multidrug-resistant bacteria are a global concern. The unique nature of silver as a powerful antimicrobial agent is proven in modern medicine [4]. Nanoscience is one such field that is being widely explored to further enhance silver's antimicrobial activity, as AgNPs possess a large surface area-to-volume ratio [5]. Research studies have shown that AgNPs display a wide range of bioactivities, including anti-plasmodial [6], anticancer [7], antimicrobial [8][9], anti-inflammatory, antioxidant, anti-diabetic [9], and anti-platelet properties [10]. Beyond pharmacological applications, the antimicrobial capabilities of AgNPs can also be explored for applications in environmental remediation. Water purification is one such area where microbial contamination remains a significant concern. In India, groundwater is a vital resource for domestic and industrial purposes that is prone to contamination from fecal contaminants, pesticides, chemicals, and industrial activities [11]. Consequently, controlling microbial contamination in water is vital for preventing harmful diseases

## Publisher's Note:

Pandawa Institute stays neutral with regard to jurisdictional claims in published maps and institutional affiliations.



## Copyright:

© 2025 by the author(s).

Licensee Pandawa Institute, Metro, Indonesia. This article is an open access article distributed under the terms and conditions of the Creative Commons Attribution (CC BY) license (<https://creativecommons.org/licenses/by/4.0/>).

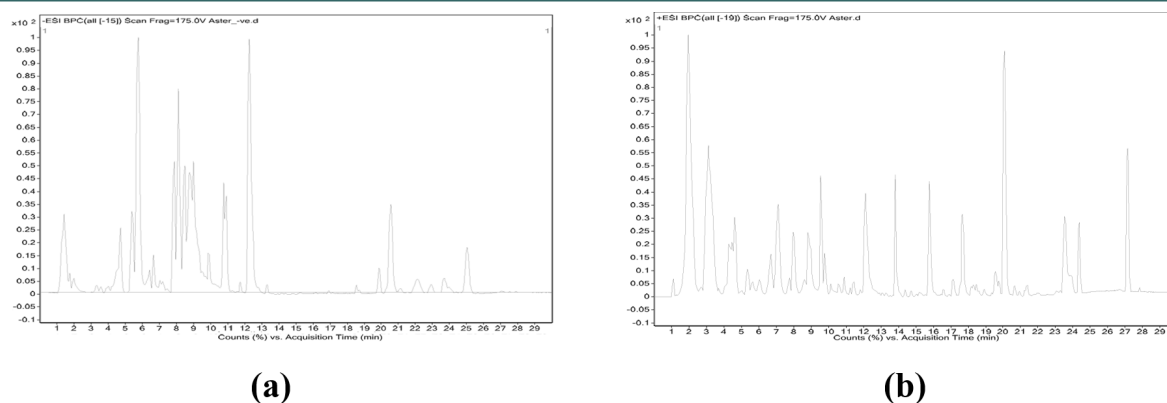


**Figure 1.** LC-HRMS chromatogram for (a) positive and (b) negative ESI of AFW.

such as gastroenteritis, cholera, dysentery, and diarrhea [12][13], requiring efficient and immediate treatment solutions, such as the use of nanoparticles.

Several physical and chemical methods have been used to produce AgNPs, but these methods often involve the use of toxic agents that pose a risk to the environment [14][15]. As an alternative, green synthesis has gained considerable attention owing to their low cost, scalability and eco-friendly nature. This approach uses plant extracts or microorganisms as reducing and stabilizing agents. While nanoparticle synthesis using microbes such as yeast, fungi and bacteria are effective, they face several drawbacks due to their elaborate procedures and numerous purification steps [16]. In contrast, plant-based synthesis is simpler, more rapid, cost-effective and produces nanoparticles with diverse shapes and sizes [16]-[18]. The efficiency of plant extracts can be attributed to biomolecules like phenolic compounds, proteins, tannins, and flavonoids which act as capping and reducing agents in nanoparticle synthesis [19][20].

Most research studies on phyto-fabricated nanoparticles have focused on fresh plant material. However, large-scale commercial synthesis of nanoparticles would require vast quantities of fresh plants, raising sustainability concerns. Utilizing organic waste, particularly floral waste, over their fresh counterparts could be a more practical approach for the large-scale biosynthesis of AgNPs. In India, flowers such as aster, marigold, and rose, which hold a key place in auspicious occasions, are often improperly discarded, fostering the breeding of harmful microorganisms and environmental issues [21]. Estimates suggest that approximately

4.74 million tonnes of floral waste are generated daily in India [22]. Previous studies by the authors have demonstrated the potential of aster floral waste in applications such as pH indication, antioxidant activity, and DNA damage protection [23][24]. To date, only one study has used temple floral waste, including *Aegle marmelos*, and *Tagetes erecta* flowers and leaves, to synthesize AgNPs for detecting Cr(VI) in water [25]. However, to the best of our knowledge, no studies have explored the versatile applications of aster floral waste-derived AgNPs in combating bacterial growth, inhibiting cancer cell proliferation, and decontaminating groundwater.

Based on the rationale stated above, the present study aimed to explore the multipurpose applications of AgNPs synthesized by upcycling AFW using a microwave-assisted approach. Specifically, the study aimed to: (i) evaluate their antibacterial activity, (ii) investigate their environmental application in mitigating coliform growth in borewell water, and assess changes in the physicochemical parameters of the water post-treatment, and (iii) evaluate cytotoxicity of AgNPs on cancer and normal human cell lines.

## 2. MATERIALS AND METHODS

### 2.1. Materials

Waste light and dark pink-hued aster [*Callistephus chinensis* (L.)] flowers were obtained from local markets in Mumbai. Both nutrient broth and nutrient agar were procured from HiMedia laboratories, Mumbai. Gram-negative bacteria, i.e., *E. coli* (ATCC 8739) and *P. aeruginosa* (ATCC 9027), and Gram-positive bacteria, i.e., *S. aureus*

**Table 1.** LC-HRMS data for aqueous extract of AFW.

Name	Formula	Mass	m/z	RT
HR-LCMS chromatogram (Negative ESI)				
Isocitrate	C <sub>6</sub> H <sub>8</sub> O <sub>7</sub>	192.0273	191.0200	1.771
Quinic acid	C <sub>7</sub> H <sub>12</sub> O <sub>6</sub>	192.0627	191.0555	4.741
Benzoic acid	C <sub>7</sub> H <sub>6</sub> O <sub>2</sub>	122.0362	167.0346	5.900
<i>m</i> -Coumaric acid	C <sub>9</sub> H <sub>8</sub> O <sub>3</sub>	164.0471	163.0399	10.245
Quercitrin	C <sub>21</sub> H <sub>20</sub> O <sub>11</sub>	448.1008	507.1150	6.786
Kaempferol	C <sub>15</sub> H <sub>10</sub> O <sub>6</sub>	286.0478	285.0406	12.532
Luteolin	C <sub>15</sub> H <sub>10</sub> O <sub>6</sub>	286.0478	285.0406	12.532
Baicalein	C <sub>15</sub> H <sub>10</sub> O <sub>5</sub>	270.0530	269.0456	9.005
alpha-Licanic acid	C <sub>18</sub> H <sub>28</sub> O <sub>3</sub>	292.2034	291.1958	19.501
Gallic acid	C <sub>7</sub> H <sub>6</sub> O <sub>5</sub>	170.0210	169.0137	2.853
Caffeic acid	C <sub>9</sub> H <sub>8</sub> O <sub>4</sub>	180.0418	179.0345	8.723
Enol-phenylpyruvate	C <sub>9</sub> H <sub>8</sub> O <sub>3</sub>	164.0471	163.0399	10.245
Vanillic acid	C <sub>8</sub> H <sub>8</sub> O <sub>4</sub>	168.0418	167.0346	6.364
3-hydroxy-4-methoxymandelate	C <sub>9</sub> H <sub>10</sub> O <sub>5</sub>	198.0527	197.0456	4.542
Chlorogenic acid	C <sub>16</sub> H <sub>18</sub> O <sub>9</sub>	354.0939	353.0866	24.693
Isoferulic acid	C <sub>10</sub> H <sub>10</sub> O <sub>4</sub>	194.0577	193.0508	10.01
Ellagic acid	C <sub>14</sub> H <sub>6</sub> O <sub>8</sub>	302.0063	300.999	8.577
Resorcinol	C <sub>6</sub> H <sub>6</sub> O <sub>2</sub>	110.0366	109.0293	4.434
Gentisic acid	C <sub>7</sub> H <sub>6</sub> O <sub>4</sub>	154.0266	153.0193	4.434
Enol-phenylpyruvate	C <sub>9</sub> H <sub>8</sub> O <sub>3</sub>	164.0471	163.0399	10.245
Malic acid	C <sub>4</sub> H <sub>6</sub> O <sub>5</sub>	134.0216	133.0143	1.493
4-Oxovalproic acid	C <sub>8</sub> H <sub>14</sub> O <sub>3</sub>	158.0941	157.0868	7.291
Elenaic acid	C <sub>11</sub> H <sub>14</sub> O <sub>6</sub>	242.0782	241.0708	15.853
Arbutin	C <sub>12</sub> H <sub>16</sub> O <sub>7</sub>	272.0890	271.0818	9.087
Azelaic acid	C <sub>9</sub> H <sub>16</sub> O <sub>4</sub>	188.1047	187.0975	9.187
3-Dehydro-L-gulonate	C <sub>6</sub> H <sub>10</sub> O <sub>7</sub>	194.0427	193.0354	1.225
Chlorogenic acid	C <sub>16</sub> H <sub>18</sub> O <sub>9</sub>	354.0965	353.0891	4.653
Quinic acid	C <sub>7</sub> H <sub>12</sub> O <sub>6</sub>	192.0631	191.0558	5.571
Isobiflorin	C <sub>16</sub> H <sub>18</sub> O <sub>9</sub>	354.0949	353.0876	5.653
5,7-Dihydroxychromone	C <sub>9</sub> H <sub>6</sub> O <sub>4</sub>	178.0259	177.0187	6.333
Neoastilbin	C <sub>21</sub> H <sub>22</sub> O <sub>11</sub>	450.1156	449.1085	6.498
Quercetin 3-rhamnoside-7-glucoside	C <sub>27</sub> H <sub>30</sub> O <sub>16</sub>	610.1537	609.1463	7.875
Myricitrin	C <sub>21</sub> H <sub>20</sub> O <sub>12</sub>	464.0955	463.0883	8.063
Catechin-(4alpha)-gallocatechin-(4alpha)-catechin	C <sub>45</sub> H <sub>38</sub> O <sub>19</sub>	882.1916	927.1904	8.132
Epiafzelechin-(4beta)-epicatechin 3,3'-digallate	C <sub>44</sub> H <sub>34</sub> O <sub>19</sub>	866.1563	925.1713	8.143
Quercetin 3-O-glucuronide	C <sub>21</sub> H <sub>18</sub> O <sub>13</sub>	478.0741	477.0669	8.209
3-Methylellagic acid 8-rhamnoside	C <sub>21</sub> H <sub>18</sub> O <sub>12</sub>	462.0792	461.0719	8.231
Glyphoside	C <sub>23</sub> H <sub>22</sub> O <sub>13</sub>	506.1075	505.1002	8.527

**Table 1.** *Cont.*

Name	Formula	Mass	m/z	RT
<b>HR-LCMS chromatogram (Negative ESI)</b>				
Quercetin 3- <i>O</i> -malonylglucoside	C <sub>24</sub> H <sub>22</sub> O <sub>15</sub>	550.0956	549.0883	8.605
Luteolin 4'- <i>O</i> -glucoside	C <sub>21</sub> H <sub>20</sub> O <sub>11</sub>	448.1012	447.0939	8.704
Chlorogenic acid	C <sub>16</sub> H <sub>18</sub> O <sub>9</sub>	354.0951	353.0879	8.737
Baicalin	C <sub>21</sub> H <sub>18</sub> O <sub>11</sub>	446.0850	445.0776	9.020
Irisolidone 7- <i>O</i> -glucuronide	C <sub>23</sub> H <sub>22</sub> O <sub>12</sub>	490.1134	489.1068	9.354
Sennoside F	C <sub>44</sub> H <sub>38</sub> O <sub>23</sub>	934.1854	979.184	9.357
Genistein	C <sub>15</sub> H <sub>10</sub> O <sub>5</sub>	270.0530	269.0458	9.815
Baicalin	C <sub>21</sub> H <sub>18</sub> O <sub>11</sub>	446.0851	445.0777	10.114
Proanthocyanidin A5'	C <sub>30</sub> H <sub>24</sub> O <sub>12</sub>	576.1264	575.1193	10.758
Fustin	C <sub>15</sub> H <sub>12</sub> O <sub>6</sub>	288.0637	287.0564	10.783
Neryl arabinofuranosyl-glucoside	C <sub>21</sub> H <sub>36</sub> O <sub>10</sub>	448.2307	493.229	10.842
Lauryl hydrogen sulfate	C <sub>12</sub> H <sub>26</sub> O <sub>4</sub> S	266.1548	265.1475	20.426
Tributyl phosphate	C <sub>12</sub> H <sub>27</sub> O <sub>4</sub> P	266.1642	265.1569	20.776
Salannin	C <sub>34</sub> H <sub>44</sub> O <sub>9</sub>	596.2992	595.2919	22.210
Valdiate	C <sub>17</sub> H <sub>26</sub> O <sub>5</sub>	310.1803	309.1731	22.946
<b>HR-LCMS chromatogram (Positive ESI)</b>				
Isopentyl gentiobioside	C <sub>17</sub> H <sub>32</sub> O <sub>11</sub>	412.1952	413.2028	1.079
1-Pyrenylsulfate	C <sub>16</sub> H <sub>10</sub> O <sub>4</sub> S	298.0300	299.0380	1.094
Tryptophyl-alanine	C <sub>14</sub> H <sub>17</sub> N <sub>3</sub> O <sub>3</sub>	275.1288	276.1358	1.883
Phenylalanyl-gamma-glutamate	C <sub>14</sub> H <sub>19</sub> N <sub>3</sub> O <sub>4</sub>	293.1382	294.1453	1.884
2-[4-(3,4-Methylenedioxyphenyl)butyl]-4(1 <i>H</i> )-quinolinone	C <sub>20</sub> H <sub>19</sub> NO <sub>3</sub>	321.1362	344.1255	1.897
Tryptophyl-alanine	C <sub>14</sub> H <sub>17</sub> N <sub>3</sub> O <sub>3</sub>	275.1284	276.1355	2.193
Benzosimuline	C <sub>20</sub> H <sub>19</sub> NO <sub>2</sub>	305.1432	328.1326	2.868
6-(Pentylthio)purine	C <sub>10</sub> H <sub>14</sub> N <sub>4</sub> S	222.0952	223.1023	2.914
Benzosimuline	C <sub>20</sub> H <sub>19</sub> NO <sub>2</sub>	305.1423	328.1318	3.585
Phenylalanyl-arginine	C <sub>15</sub> H <sub>23</sub> N <sub>5</sub> O <sub>3</sub>	321.1835	322.1914	4.103
<i>N</i> 2-(2-Carboxymethyl-2-hydroxysuccinoyl)arginine	C <sub>12</sub> H <sub>20</sub> N <sub>4</sub> O <sub>8</sub>	348.1247	349.1320	4.308
7-beta-D-Glucopyranosyloxybutyridenephthalide	C <sub>18</sub> H <sub>22</sub> O <sub>8</sub>	366.1354	367.1431	4.313
2-Oxo-8-methylthiooctanoic acid	C <sub>9</sub> H <sub>16</sub> O <sub>3</sub> S	204.0849	205.0923	4.566
<i>N</i> 2-(2-Carboxymethyl-2-hydroxysuccinoyl)arginine	C <sub>12</sub> H <sub>20</sub> N <sub>4</sub> O <sub>8</sub>	348.1245	349.1318	4.639
Absciscic acid glucose ester	C <sub>21</sub> H <sub>30</sub> O <sub>9</sub>	426.1887	427.1963	5.046
Kuwanon R	C <sub>40</sub> H <sub>38</sub> O <sub>9</sub>	662.2596	663.2682	5.378
Benz[ <i>a</i> ]acridine	C <sub>17</sub> H <sub>11</sub> N	229.0903	252.0797	5.600
Scorzoside	C <sub>21</sub> H <sub>30</sub> O <sub>8</sub>	410.1932	411.2012	6.377
Heliannone B	C <sub>17</sub> H <sub>16</sub> O <sub>5</sub>	300.1027	301.1100	6.634
6-Deoxyjacareubin	C <sub>18</sub> H <sub>14</sub> O <sub>5</sub>	310.0871	311.0947	7.466
6"-Caffeoylisorientin	C <sub>30</sub> H <sub>26</sub> O <sub>14</sub>	610.1377	611.1453	7.789
6-O-Galloylsucrose	C <sub>19</sub> H <sub>26</sub> O <sub>15</sub>	494.1238	517.1196	8.478

**Table 1.** *Cont.*

Name	Formula	Mass	m/z	RT
<b>HR-LCMS chromatogram (Positive ESI)</b>				
Aspartyl-Aspartate	C <sub>8</sub> H <sub>12</sub> N <sub>2</sub> O <sub>7</sub>	248.0635	271.0525	8.893
Orotidine	C <sub>10</sub> H <sub>12</sub> N <sub>2</sub> O <sub>8</sub>	288.0566	289.0641	10.576
Oxopurpureine	C <sub>21</sub> H <sub>19</sub> NO <sub>6</sub>	381.1228	404.1125	16.617
Echimidine	C <sub>20</sub> H <sub>31</sub> NO <sub>7</sub>	397.2140	398.2208	24.326

(ATCC 6538) were procured from Kwik-Sticks™ Microbiologics, USA. The human dermal fibroblast (HDF) primary culture was obtained from juvenile foreskin, sourced from HiMedia Laboratories, Mumbai, India. The HeLa cell line was procured from the National Centre for Cell Science, Pune. Both the HeLa and HDF cells were cultured in Dulbecco's Modified Eagle Medium (DMEM) procured from HiMedia laboratories, India, supplemented with 10% fetal bovine serum (FBS, Gibco, Thermo Scientific, USA) and 1% penicillin-streptomycin antibiotic solution (HiMedia laboratories, India). All other chemicals were of analytical grade or LC-MS grade. The ELISA plate reader used was of Thermo Lab Systems with MRX revealer software.

## 2.2. Methods

### 2.2.1. Preparation of Aster Floral Waste Extract

The petals were washed and shade dried. AFW extract was prepared by boiling 5 g of dried aster petals in 50 mL distilled water for 2 min. The extract was cooled and filtered using muslin cloth.

### 2.2.2. Phytochemical Analysis of AFW Extract

The extract prepared for synthesis of AgNPs was analyzed for total phenolic content (TPC) and total flavonoid content (TFC), whereas LC-HRMS was performed at IIT Bombay, SAIF. TPC analysis was conducted as per a previous procedure with minor modifications [26]. The extract was diluted in water in a ratio of 1:10. Gallic acid was used as a standard for TPC. For TPC, a total of 20 µL of the crude AFW extract or distilled waste or gallic acid standard was added to 100 µL of 7.5% Na<sub>2</sub>CO<sub>3</sub> in a 96-well plate. The plate was incubated for 10 min and followed by the addition of 100 µL of Follin-Ciocalteu (1:10) reagent. The plate was further

incubated for 10 min at room temperature. The absorbance was read at 750 nm and result was expressed as mg of gallic acid equivalent TPC present in the total AFW extract [27].

TFC analysis was conducted as per the methodology given by Chlopicka et al. (2012). To 100 µL of the AFW extract (1:10 in water) or different concentration of quercetin standard was added to 6 µL 10% AlCl<sub>3</sub> and incubated for 5 min. Further 6 µL of 5% NaNO<sub>2</sub> was added to the plate and further incubated for 5 min. Lastly, 40 µL of 1M NaOH was added to the wells and volume was made up to 200 µL using distilled water. The plates were incubated at room temperature for further 30 min. The absorbance was read at 415 nm and result was expressed as mg of quercetin equivalent TFC present in total AFW extract [28].

### 2.2.3. Green Synthesis and Purification of AgNPs

Green synthesis of AgNPs was performed by adding 5 mL AFW extract and 15 mL of 5 mM AgNO<sub>3</sub> solution to 30 mL distilled water. This mixture was heated in a microwave at 600 W for 2 min followed by incubation in dark at room temperature for 24 h. The nanoparticles were purified by centrifugation of the as-synthesized AgNPs at 10,000 rpm for 10 min [15]. The pellet was resuspended in dechlorinated distilled water, and the process was repeated until a clear supernatant was observed. This pellet was then collected and air-dried in the dark. The presence of AgNPs was confirmed spectrophotometrically by analyzing the absorbance spectra using Cary 50 UV-Visible spectrophotometer.

### 2.2.4. Characterization of Biosynthesized AgNPs

Characterization of purified AgNPs using Fourier transform-infrared (FT-IR) spectroscopy, transmission electron microscopy (TEM), selected

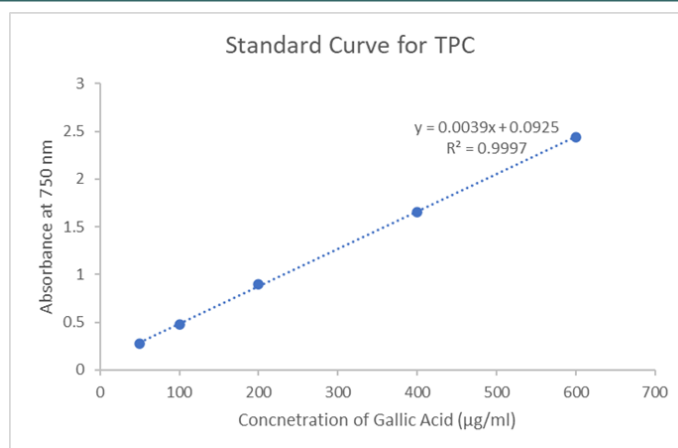


**Figure 2.** Standard calibration curve of gallic acid for determining the total phenolic content of aqueous AFW extract.

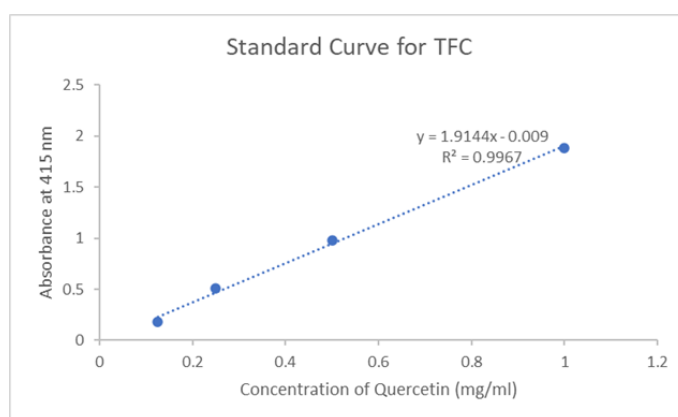


**Figure 3.** Standard calibration curve of quercetin for determining the total flavonoid content of aqueous AFW extract.

area electron diffraction (SAED) pattern analysis, X-ray diffraction (XRD) and scanning electron microscopy (SEM) was performed at Sophisticated Analytical Instrumentation Facility (SAIF) at IIT Bombay, India. FT-IR analysis of AFW extract and purified AgNPs was done using a Bruker Vertex 80, 3000 Hyperion microscope with FT-IR system to identify the functional groups involved in nanoparticle synthesis. XRD (Panalytical Empyrean Powder Diffractometer with Cu K alpha radiation at 1.54184 Å) was performed for evaluating the crystalline structure of biosynthesized AgNPs. Field emission Gun-SEM was carried out using Jeol JSM-7600F FEG-SEM for determining the shape of the nanoparticles. FEG-TEM 300 kV was used for TEM and SAED pattern analysis for analyzing the structure and size of AgNPs [27]. Energy dispersive X-ray (EDX) analysis was conducted to confirm the presence of silver in the purified nanoparticles.

#### 2.2.5. Estimation of Minimum Inhibitory Concentration 90 (MIC90) and Minimum Bactericidal Concentrations (MBC)

The broth microdilution method is widely regarded as the gold standard for quantitatively assessing the antimicrobial activity of a sample. It helps in determining the minimum inhibitory concentration (MIC), which is the lowest concentration required to inhibit microbial growth. MIC90 refers to the MIC needed to inhibit 90% of microorganisms. To evaluate the minimum bactericidal concentration (MBC), concentrations exceeding the MIC were subsequently cultured on fresh media, allowing assessment of the lowest concentration necessary to completely eliminate the microorganisms [28].

MIC90 and MBC of biosynthesized AgNPs were tested against *E. coli*, *P. aeruginosa*, and *S. aureus*. Broth microdilution method was used to perform the MIC assay as per the procedure mentioned



previously with slight modifications [29]. Nanoparticle stock solution (1 mg/mL) was prepared in sterile nutrient broth (NB) followed by 15 min sonication. Different concentrations of purified AgNPs ranging from 1–0.015625 mg/mL were prepared by two-fold serial dilutions. Next, 100  $\mu$ L of these serially diluted AgNPs were dispensed in 96-well microtiter plates followed by the addition of 10  $\mu$ L microbial culture (0.5 McFarland fresh bacterial culture with  $1.5 \times 10^8$  CFU/mL). Color blanks for the samples were set up by adding 100  $\mu$ L of the respective nanoparticle concentrations to 10  $\mu$ L sterile NB. The negative control or growth control consisted of 100  $\mu$ L sterile NB and 10  $\mu$ L microbial suspension. All tests and control samples were prepared in triplicates and incubated at 37 °C for 24 h. The test microtiter plate was read at 630 nm in ELISA plate reader. MBC was assessed by adding 100  $\mu$ L of concentrations starting from MIC90 till the highest (1 mg/mL) were cultured on sterile nutrient agar plates and incubated further at 37 °C for 24 h. The MBC was termed as the minimal concentration of AgNPs which completely killed the microorganisms with no evident bacterial growth seen on the nutrient agar plate after incubation [29].

#### 2.2.6. Effect of AgNPs on Growth of Coliforms in Borewell Water

The microbicidal activity of AgNPs was further extended to assess its ability to control and eliminate the growth of coliforms in borewell water. Borewell water samples were collected from Thane, Maharashtra, India, and stored below 8 °C during transit to prevent the growth of any

microorganisms. The water sample (300 mL) was treated with 0.1 mg/mL of AgNPs. The sample was incubated in the dark on a rotary shaker at 1000 rpm. After 24 h incubation, the AgNPs were separated by centrifugation for 20 min at 5000 rpm. The quality of nanoparticle-treated and untreated water samples was assessed through tests such as turbidity, total solids, pH, temperature, alkalinity, biological oxygen demand (BOD), most probable number (MPN) of coliforms, and chemical oxygen demand (COD) [30][31]. The treated water sample was plated on sterile endo agar media for confirmation of MPN analysis.

#### 2.2.7. Cytotoxic Analysis of AgNPs on HeLa and HDF Cell Lines

The anticancer effects of the biosynthesized AgNPs were evaluated using two cell cultures: HDF and HeLa cell lines. This dual-cell line strategy allows for assessing the AgNPs' ability to specifically target cancerous cells while minimizing damage to normal cells. Cells were trypsinized using 1X trypsin and seeded in a 96-well microtiter plate at a cell density of  $5.0 \times 10^3$  cells/well. The plate was then incubated at 37 °C in a humidified 5% CO<sub>2</sub> incubator for 24 h [32]. Existing media was removed post-incubation and 100  $\mu$ L purified AgNPs were added to each well in a two-fold serial dilution to obtain final concentrations between 0.015625–0.5 mg/mL. All the dilutions were performed in triplicates. Cells treated with only the medium, i.e., without AgNPs, served as media control or 100% cell viability control. The plates were again incubated for 24 h. After incubation, cell viability was analyzed using SRB staining assay,

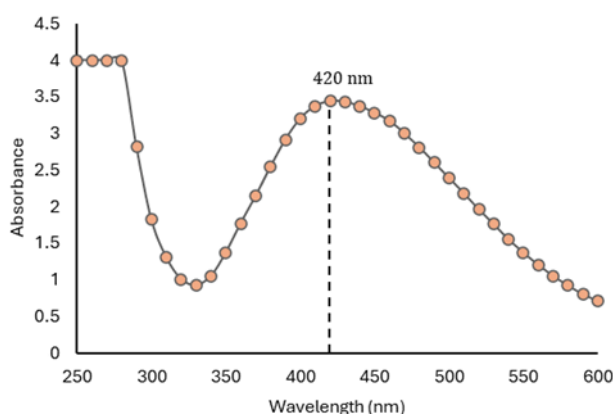


**Figure 4.** UV-visible spectrum indicating SPR absorption of biosynthesized AgNPs.

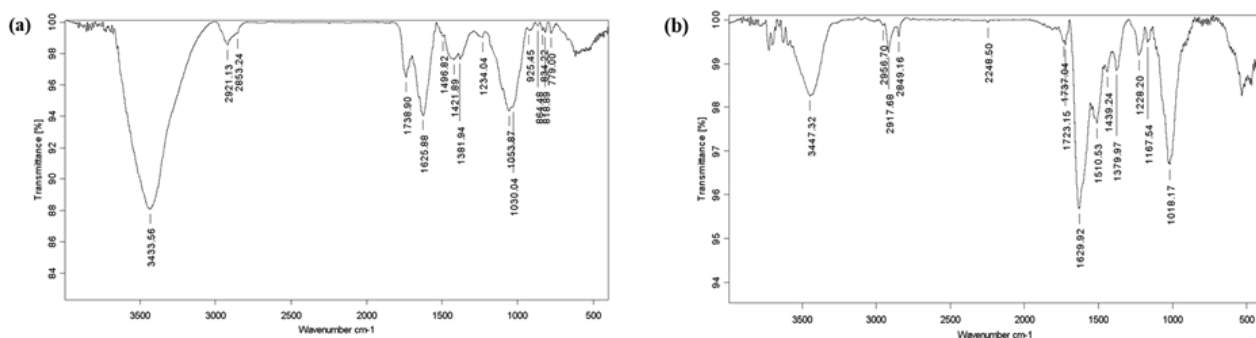


**Figure 5.** FT-IR spectra of (a) AFW extract and (b) biosynthesized AgNPs.

and the readings were obtained at 530 nm using ELISA plate reader [33]. Cell viability was calculated using Eq. (1).

$$\text{Cell viability} = \frac{\text{Average absorbance of Treatment} \times 100}{\text{Average absorbance of 100\% cell viability control}} \quad (1)$$

### 2.2.8. Statistical Analysis

Comparison of mean values was performed using one-way ANOVA with JASP Team (2025, version 0.19.3) statistical software. Nanoparticle sizes analyzed using characterization techniques were expressed as mean  $\pm$  standard error. A  $p$ -value of less than 0.05 was considered as statistically significant.

## 3. RESULTS AND DISCUSSIONS

### 3.1. Phytochemical Analysis of Aqueous AFW Extract

#### 3.1.1. LC-HRMS Analysis

The AFW extract was analyzed using LC-HRMS. In the negative ESI mode (Figure 1(a)), most detected peaks were identified as polyphenols and flavonoids, along with a smaller proportion of organic acids and alkaloids (Table 1). In contrast, the positive ESI mode (Figure 1(b)) predominantly revealed the presence of peptides, glycosides, alkaloids, and other non-phenolic compounds. These findings suggest that AFW extract is a rich source of diverse phytochemicals with potential biological significance.

#### 3.1.2. TPC and TFC Measurements

The AFW extract was analysed for its TPC and TFC. According to the Figure 2, the regression equation obtained was  $y = 0.0039x + 0.0925$ , with a high  $R^2$  of 0.9997, indicating an excellent linear fit.

The absorbance value for the 1:10 diluted extract was recorded at 0.743. Using the regression equation and accounting for the dilution factor, the TPC of the AFW extract was calculated to be 1.6687 mg of gallic acid equivalents (GAE).

Based on the data presented in Figure 3, the calibration curve for quercetin yielded a linear regression equation of  $y = 1.9144x - 0.009$ , with an  $R^2$  value of 0.9967, indicating excellent linearity. The absorbance of the AFW extract diluted at 1:10 was measured to be 1.8515. Substituting this value into the standard curve equation and correcting for the dilution factor, the TFC of the AFW extract was calculated as 9.71 mg quercetin equivalents per mL of extract.

### 3.2. UV-Visible Spectrophotometric Analysis of AgNPs

The AFW extract displayed a characteristic pink color that changed to deep brown upon the addition of  $\text{AgNO}_3$ , followed by microwave-assisted heating. This evident change in color was indicative of  $\text{Ag}^+$  reduction to  $\text{Ag}^0$ . As shown in Figure 4, UV-visible spectrophotometric analysis identified a distinct surface plasmon resonance (SPR) absorption peak at 420 nm wavelength.

### 3.3. FT-IR Analysis of AgNPs

The FT-IR spectrum of aqueous extract of aster flower petals exhibited peaks at 3433, 2921, 2853, 1739, 1626, 1422, 1382, 1234, 1054, and 1030  $\text{cm}^{-1}$ , that correspond to the functional groups, O–H, N–H, C–H, C=O, C=C, C=C aromatic, C–O–H, and C–O, respectively as seen in Figure 5(a) [34–37]. These groups may be the factors contributing to  $\text{Ag}^+$  reduction and further stabilization of AgNPs. Literature suggests that the presence of C=O, O–H, and N–H groups are involved in synthesizing the



nanoparticles by reduction of  $\text{Ag}^+$  ions to  $\text{Ag}^0$  via electron or hydrogen donation [38]–[40]. On the other hand, the groups like C–O of polysaccharide, C=C alkene, and C=C aromatic are likely to act like capping ligands for stabilizing the nanoparticles and impeding their agglomeration [41][42]. Upon closer comparison, as delineated in Figure 5(b), differences were observed between the relative peak intensities of the AFW extract and AgNPs along with a slight shift in spectrum shoulder. The biosynthesized AgNPs exhibited spectrum band shifts at 3447, 2957, 2849, 1737, 1630, 1439, 1380, 1228, and  $1018\text{ cm}^{-1}$ . Additional low-intensity peaks were observed at 2248, 1510, and  $1167\text{ cm}^{-1}$ , suggesting the presence of C≡C stretching, amide II in protein and C=O bond, respectively [43]. In summary, the peaks detected in the FT-IR analysis may be ascribed to flavonoids and phenolic compounds contributing to the capping and stabilization of the biosynthesized AgNPs [44][45].

### 3.4. EDX Analysis of Biosynthesized AgNPs

EDX analysis of nanoparticles was performed to verify the presence of elemental silver in AgNPs. As seen in Figure 6(a), a strong peak at 3 KeV was observed which confirms the presence of metallic silver in the sample [46]. Elemental mapping of total elements revealed the presence of metallic silver (66.12%), carbon (29.55%), chlorine (3.50%), and oxygen (0.83%). The higher weight percentages of metallic silver strongly suggest the presence of crystalline biosynthesized AgNPs [47]

[48]. However, the atomic percentages revealed higher values contributed by carbon (Table 2). Interestingly, the unallocated phase of the EDX spectrum showed the presence of carbon (weight % = 86.13; atomic % = 97.02), silver (weight % = 10.96; atomic% = 1.37), chlorine (weight % = 1.85; atomic%=0.71), and oxygen (weight% = 1.06%; atomic% = 0.90) were noted (Figure 6(b)). This indicates that the substrate is likely carbon-based and a contributing factor to the observed higher percentage of carbon [49]. Additionally, minor traces of oxidized silver and chlorine were noted that could originate from phytochemical residues or impurities from the method of synthesis [50].

### 3.5. XRD Analysis of Biosynthesized AgNPs

The XRD pattern observed confirmed the crystalline nature of AgNPs. As displayed in Figure 7, the distinct diffraction peaks at  $37.9^\circ$ ,  $43.9^\circ$ ,  $64.2^\circ$  and  $77.3^\circ$  were detected that respectively correspond to 111, 200, 220 and 311 planes of face-centered cubic structure (fcc) of metallic silver ( $\text{Ag}^0$ ) as per the Joint Committee on Powder Diffraction Standards file No. 04-0783. Utilizing Scherrer's equation, the average crystalline size of the green synthesized AgNPs was calculated to be 24.6 nm. In addition to these primary peaks, additional diffraction peaks at  $27.81^\circ$ ,  $31.88^\circ$ , and  $54.61^\circ$  corresponding to 100, 111, and 220 were observed (Figure 7). These peaks align closely with the characteristic diffraction peaks of silver oxide ( $\text{AgO}$ ) (JCPDS No. 01–076-1489), suggesting the

**Table 2.** Sum elemental composition of area-based EDX analysis of biosynthesized AgNPs.

Element	Weight %	Atomic %
C (Carbon)	29.55	76.31
O (Oxygen)	0.83	1.61
Cl (Chlorine)	3.50	3.07
Ag (Silver)	66.12	19.01

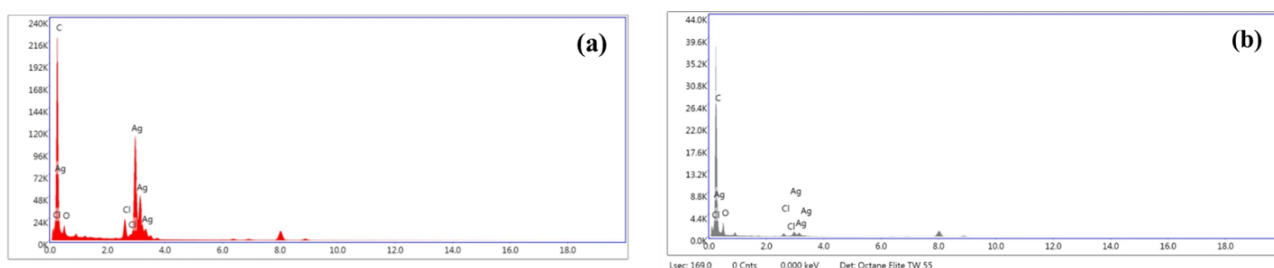


**Figure 6.** EDX analysis of (a) biosynthesized AgNPs and (b) unallocated phase of EDX spectrum.

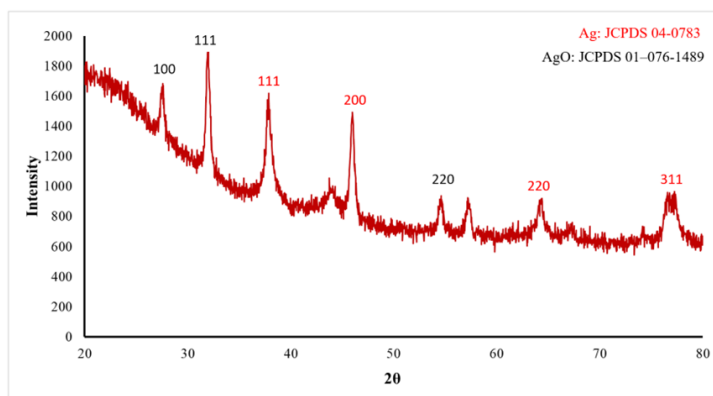


**Figure 7.** XRD pattern displaying characteristic peaks of Ag with additional peaks of AgO.

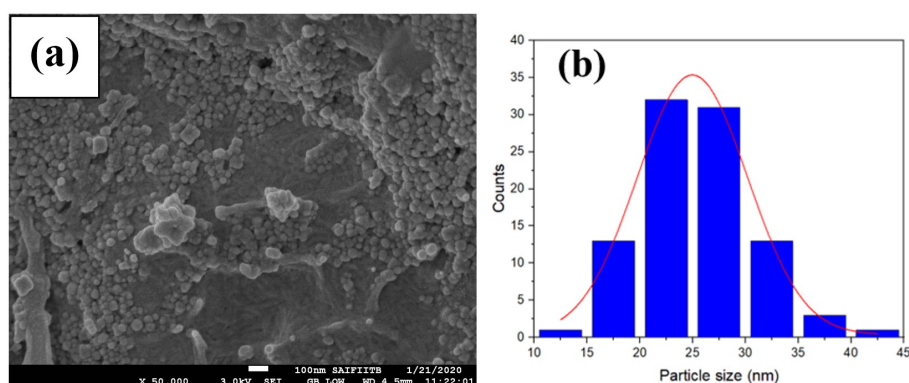


**Figure 8.** (a) SEM image and (b) particle size distribution histogram of AgNPs.

formation of AgO as a secondary phase and are indicative of the orthorhombic or tetragonal crystal structure of AgO [51]. The presence of AgO could be due to partial surface oxidation of AgNPs. Additionally, the EDX results revealed, as mentioned before, showed that the weight percentage of Ag<sup>0</sup> was more than that of oxygen, indicating that majority of the nanoparticles contain elemental silver. Hence, the results of XRD and EDX collectively indicate that the biosynthesized nanoparticle is predominantly AgNPs.

### 3.6. SEM Analysis of Biosynthesized AgNPs

Based on the SEM micrograph illustrated in Figure 8(a), it can be inferred that the green synthesized AgNPs possessed a predominantly spherical shape with minor some irregularities in shape. AgNPs of varied sizes between  $24.90 \pm 0.16$  nm were observed in the micrograph (Figure 8(b)).

### 3.7. TEM and SAED Pattern Analysis of Biosynthesized AgNPs

TEM results, as shown in Figure 9(a), further confirmed that AgNPs were predominantly

spherical with few variations in morphology. The histogram, which was generated using 112 nanoparticles, showed the average size distribution to be  $23.10 \pm 0.52$  nm (Figure 9(b)). The d-spacing of lattice fringes measured from TEM was noted to be 0.13 nm, corresponding to the (220) lattice plane of fcc silver, as seen in Figure 9(c). Furthermore, as depicted in Figure 9(d), the SAED pattern displayed distinct diffraction rings corresponding to (111), (200), (220), and (311) planes. These are in concordance with the XRD peaks observed at  $2\theta$  values of  $37.9^\circ$ ,  $43.9^\circ$ ,  $64.2^\circ$  and  $77.3^\circ$  respectively (Figure 7). The SAED results thus confirmed the face-centered cubic crystalline lattice structure of metallic silver in AgNPs.

### 3.8. Evaluation of MIC90 and MBC of Biosynthesized AgNPs

Broth microdilution test was performed for determining the MIC90 of purified AgNPs. As shown in Table 3, the MIC90 of nanoparticles against Gram-negative and Gram-positive microorganisms was found to be 0.0625 and 0.125 mg/mL AgNPs, respectively. Furthermore, the

MBC of AgNPs was evaluated by studying the nanoparticle concentration at which no growth was observed on culturing on the nutrient agar plate thus indicating their bactericidal activity. Based on the MIC90 results, nanoparticle concentrations ranging between 0.0625 and 1 mg/mL were selected for determining MBC against *E. coli* and *P. aeruginosa*. As seen in Figures 10(a) and 10(b), *E. coli* and *P. aeruginosa* did not grow in plates with nanoparticle concentrations from 0.0625 to 1 mg/mL. Thus, 0.0625 mg/mL AgNPs was concluded to be the MBC against the studied Gram-negative microorganisms. Similarly, based on the result observed in Figure 10(c), 0.5 mg/mL AgNPs was concluded to be the MBC for *S. aureus*. In summary, the biosynthesized AgNPs displayed effective bactericidal activity against both Gram-positive and gram-negative bacteria.

The observed antibacterial property could be attributed to their small size and rate of release of silver ions from the nanoparticles. Moreover, surface charge, surface area, and the availability of active facets are also known to influence the

antibacterial activity of AgNPs [52]. It is postulated that nanoparticles confer antibacterial property by disrupting the bacterial cell membrane, generating reactive oxygen species (ROS), penetrating the cell membrane, and eventually causing intracellular damage by interacting with crucial biomolecules like DNA and proteins [53][54]. Interestingly, as seen in Table 3, the biosynthesized AgNPs exhibited a stronger antibacterial effect against Gram-negative bacteria as compared to Gram-positive bacteria. This finding is in line with previous research studies [55]. The observed difference could be attributed to the difference in the molecular organization of the bacterial cell walls [56]. Gram-negative microorganisms possess an additional outer cell membrane that consists of negatively charged polyanionic lipopolysaccharides. This membrane is the main component that confers resistance to numerous antibiotics [57]. The present study speculates that the AgNPs might be able to overcome this resistance, since the positively charged  $\text{Ag}^+$  ions released by AgNPs can attach and perforate these

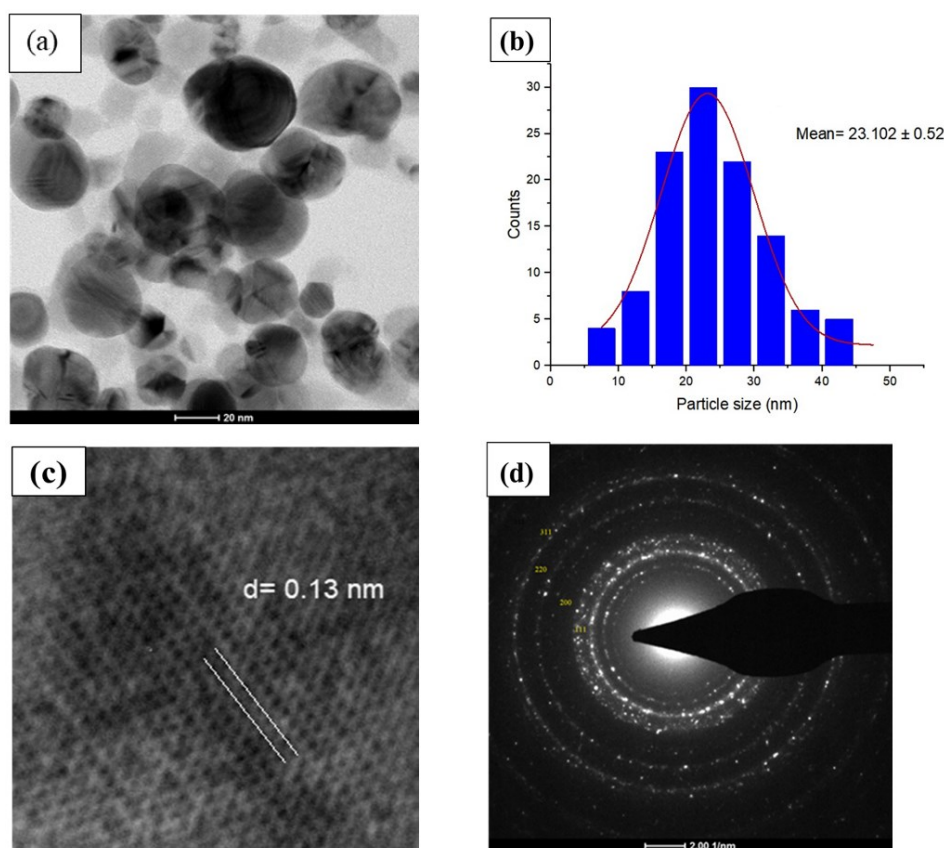


**Figure 9.** (a) TEM image, (b) particle size distribution histogram, (c) d-lattice spacing of silver nanostructure, and (d) SAED pattern of biosynthesized AgNPs.

**Table 3.** Inhibitory effect of varied concentrations of AgNPs on the growth of *E. coli*, *P. aeruginosa*, and *S. aureus*.

Biosynthesized AgNPs concentration (mg/mL)	Percent growth inhibition (%)		
	<i>E. coli</i>	<i>P. aeruginosa</i>	<i>S. aureus</i>
1	100**	100*	100**
0.5	100**	100 **	100**
0.25	98.08**	100 **	95.32**
0.125	95.45**	99.07**	90.63**
0.0625	94.74**	97.41 **	35.01*
0.03125	80.75**	18.93	19.20
0.015625	42.11*	16.89	9.48

\*\*indicates  $p < 0.01$  and \* indicates  $p < 0.05$  as compared to the growth control indicating 100% bacterial population when the means were compared using ANOVA Post Hoc Tukey Analysis.

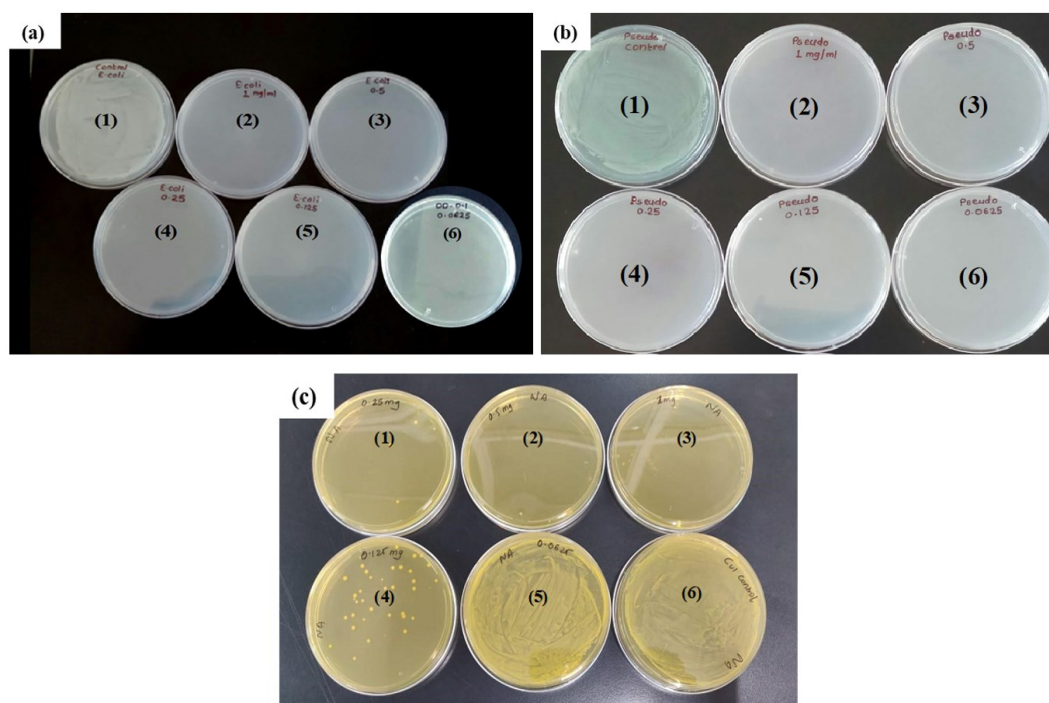


**Figure 10.** MBC analysis using different nanoparticle concentrations against (a) *E. coli* [plate (1)- negative control, plate (2)- 1mg/mL, plate (3)- 0.5 mg/mL, plate (4)- 0.25 mg/mL, plate (5)- 0.125 mg/mL, plate (6)- 0.0625 mg/mL]; (b) *P. aeruginosa* [plate (1)- negative control, plate (2)- 1 mg/mL, plate (3)- 0.5 mg/mL, plate (4)- 0.25 mg/mL, plate (5)- 0.125 mg/mL, plate (6)- 0.0625 mg/mL], and (c) *S. aureus* [plate (1)- 0.25 mg/mL, plate (2)- 0.5 mg/mL, plate (3)- 1 mg/mL, plate (4)- 0.125 mg/mL, plate (5)- 0.0625 mg/mL, plate (6)- negative control].

outer membranes through strong interactions with the negatively charged groups localized therein [58]. This in effect can reduce the chances of bacteria developing resistance against AgNPs. Such a peculiar nature of AgNPs makes them a promising agent against antibiotic-resistant gram-negative microorganisms.

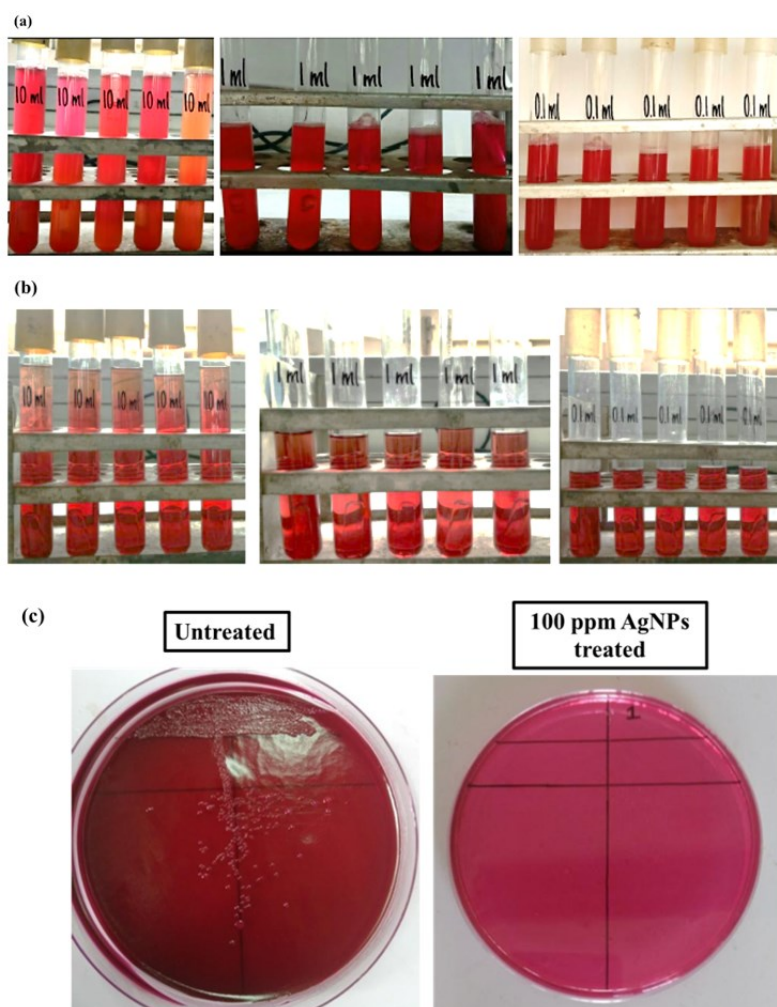
### 3.9. Effect of AgNPs on Coliform Growth in Borewell Water Sample

As indicated by the results mentioned above, the biosynthesized AgNPs displayed promising antibacterial activities. Considering this, the study further assessed the application of AgNPs in decontamination of borewell water. Research in India has shown that most physicochemical



parameters of borewell water are within the ISI permissible limits but often exceeds the WHO recommended limit for bacterial contamination [59]. It can be seen in Figure 11(a) that the untreated borewell water sample showed visible acid production and color change of the MacConkey's medium from red to yellow. Additionally, gas production was seen in all the inverted Durham's tubes. The production of gas in water indicates the presence of fecal coliforms. From the reference McCarty's chart and data obtained for untreated water sample, the coliform count of the borewell water was found to be more than 1600 CFU/100 mL. The permissible limit for fecal coliforms in safe potable water is 'no detectable presence' [60]. The presence of coliforms in borewell water was further confirmed by a confirmatory test that revealed the presence of

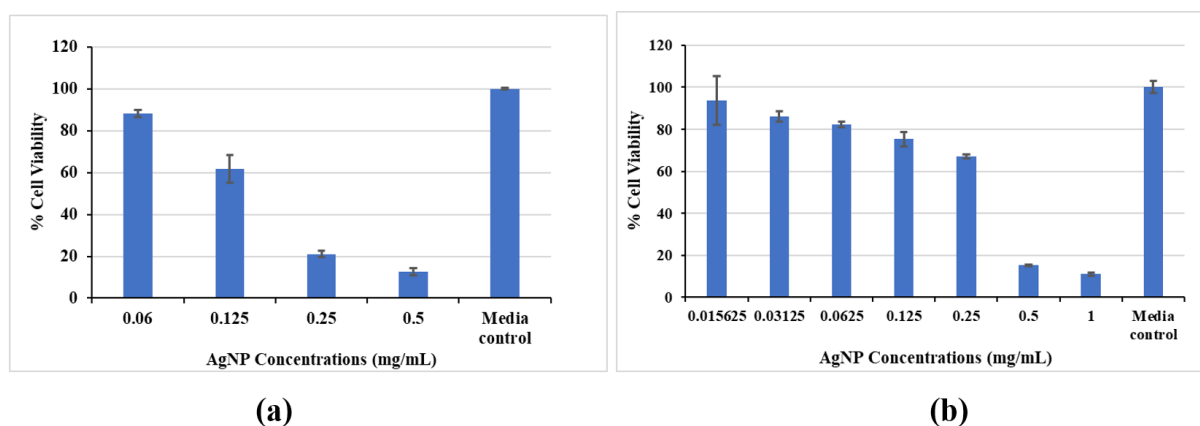
pink-colored colonies on differential endo agar medium as shown in Figure 11(c). The treatment of the contaminated borewell water sample with AgNPs resulted in no coliform growth as evidenced by the MPN analysis and confirmatory test on endo agar medium displayed in Figures 11(b) and 11(c), respectively. These results reveal the highly potent antimicrobial nature of the biosynthesized AgNPs in decontamination of borewell water. Additionally, the untreated and treated borewell water sample were assessed for any change in the physicochemical properties that may have been caused by the AgNPs during treatment. Table 4 presents a comparison between nanoparticle-treated and untreated water samples. It was observed that the treatment of borewell water sample with biosynthesized AgNPs did not alter the physicochemical properties of the water sample



**Figure 11.** (a) Color change and gas production observed in untreated water sample, (b) no change in color or gas production in nanoparticle-treated water sample, and (c) confirmatory test of untreated and nanoparticle-treated water samples using endo agar differential media.

**Table 4.** Physicochemical properties of untreated and nanoparticle treated water.

Parameter	Untreated contaminated water sample	AgNPs treated water sample	Permissible limit
pH	8.26	8.30	6.5–8.5
Temperature	32°C	32.5°C	-
Alkalinity (mg/mL)	19	20	80–120 mg/mL
Turbidity (mg/mL)	0.01	0.02	0.4–1.0 mg/mL
BOD (mg/mL)	1.0	0.6	1–2 mg/mL
DO (mg/mL)	7	8	3–8 mg/mL
COD (mg/mL)	30	15	75–100 mg/mL
Total solids (g)	0.05	0.10	100

**Figure 12.** Effect of different concentrations of AgNPs on cell viability of (a) HeLa and (b) HDF cell lines.

beyond their permissible limits. The current study thus establishes a unique feature of floral waste-mediated biosynthesized AgNPs in eradicating coliforms during water treatment. Additionally, scaling up their use to mitigate coliform contamination in borewell water through a larger-scale system holds a significant promise. Further studies on the reusability of AgNPs recovered from the treated water sample are warranted. Moreover, evaluating the efficiency of biosynthesized AgNPs in industrial effluent treatment, along with the development of cost-effective techniques such as immobilization, could further enhance their applicability.

### 3.10. Cytotoxicity of Biosynthesized AgNPs

The anticancer activity of biosynthesized AgNPs was determined against HeLa cell lines using SRB staining assay, a method based on the measurement of cellular protein content [32]. For this, the  $IC_{50}$  values were determined which indicated the concentration of nanoparticles that resulted in reduction of the cell viability by 50% as compared

to the untreated media control. The  $IC_{50}$  is a commonly determined measure in pharmacology that highlights the potency of an agent. Recently, the effects of biosynthesized AgNPs have been reported against HeLa cell lines [61]. However, an approach adopting the use of AgNPs synthesized from Indian floral waste as anticancer agents has not been explored till date. As shown in Figure 12 (a), the floral waste-based nanoparticles showed anticancer activity in a dose dependent manner against HeLa cell line with an  $IC_{50}$  of 0.21 mg/mL. Similar dose dependent effects of purified AgNPs were observed on normal HDF cells, as illustrated in Figure 12(b). However, in this case, the  $IC_{50}$  value was found to be 0.414 mg/mL. This concentration is higher than the  $IC_{50}$  value against HeLa cell line and MIC90 of biosynthesized AgNPs against the studied microorganisms. This indicates that both the anticancer  $IC_{50}$  and antibacterial MIC90 of AgNPs are not cytotoxic to normal HDF cell line.

The inherent anticancer properties of the AgNPs may stem from several mechanisms. One such



example being the release of  $\text{Ag}^+$  ions and generation of reactive oxygen species after the nanoparticles enter the cells. This has been shown to cause intense cellular damage and ultimately cell death [4]. In a research study conducted by Hussein et al. [62], the  $\text{IC}_{50}$  value of biosynthesized AgNps (*Catharanthus roseus* leaves extract) against HeLa229 cell line was found to be 0.0644 mg/mL at 24 h, while 50% inhibition was observed at a concentration of 0.0445 mg/mL after 48 h. In another study, AgNPs synthesized using *Rhizophora apiculata* aqueous leaf extract as a reducing agent exhibited a higher  $\text{IC}_{50}$  value against embryonic kidney cells (12.135 ng) compared to HeLa cell line (38.629 ng). They were found to be three-fold toxic to HEK-293 as compared to the cervical cancer cell model HeLa [63]. Biosynthesized silver nanoparticle prepared using *Melia azedarach* as both reducing and capping agents were also tested for their anticancer properties on HeLa with an  $\text{IC}_{50}$  of 300  $\mu\text{g/mL}$  [64]. The  $\text{IC}_{50}$  values reported in the current study align with those in literature, and notably, the nanoparticles displayed selective toxicity towards cancerous in comparison to the normal cells, indicating their potential therapeutic properties. Based on these favorable findings, the biosynthesized AgNPs could be further explored in therapeutic formulations. Due to the observed promising anti-cancer activity, comprehensive *in-vivo* studies are warranted to further evaluate their biocompatibility and therapeutic efficacy.

#### 4. CONCLUSIONS

The study employed an economic, sustainable, and rapid green synthesis approach to fabricate AgNPs using AFW extract. The research rationale was to align with the idea of utilizing floral waste, available in bulk quantities, for the synthesis of nanoparticles to meet their growing commercial demand. The unique multifaceted features of our biosynthesized AgNPs- such as their antibacterial and anticancer properties along with minimal cytotoxicity to normal human cell lines- highlight their potential as effective therapeutic agents. Furthermore, these biologically synthesized AgNPs demonstrated promising environmental application

in the treatment of coliform contaminated borewell water.

#### AUTHOR INFORMATION

##### Corresponding Author

**Shruti Kakodkar** — Department of Life Sciences, Somaiya Vidyavihar University, Mumbai-400077, (India);

 [orcid.org/0000-0001-7949-8099](https://orcid.org/0000-0001-7949-8099)

Email: [shrutikakodkar3@gmail.com](mailto:shrutikakodkar3@gmail.com)

##### Authors


**Pranjali Dhawal** — Research and Development Centre, Fragrances & Flavours Association of India, Mumbai-400020 (India);

 [orcid.org/0000-0001-5781-5137](https://orcid.org/0000-0001-5781-5137)

**Janvi Kadam** — KET's V.G. Vaze College, Mumbai-400081 (India);

 [orcid.org/0000-0003-4929-476X](https://orcid.org/0000-0003-4929-476X)

**Rumanna Khan** — KET's Scientific Research Centre, V. G. Vaze College Campus, Mumbai-400081 (India);

 [orcid.org/0009-0008-6987-4095](https://orcid.org/0009-0008-6987-4095)

**Pradnya Shewale** — KET's V.G. Vaze College, Mumbai-400081 (India);

 [orcid.org/0009-0002-7102-7000](https://orcid.org/0009-0002-7102-7000)

**Tejaswi Chaukekar** — KET's V.G. Vaze College, Mumbai-400081 (India);

 [orcid.org/0009-0008-6831-6745](https://orcid.org/0009-0008-6831-6745)

##### Author Contributions

Conceptualization, Methodology, Writing-Review & Editing, S. K and P. D.; Writing-Original Draft Preparation, Formal Analysis, J. K.; Resources, R. K.; Investigation, Data Curation, P. S. and T. C.

##### Conflicts of Interest

The authors declare no conflict of interest.

##### ACKNOWLEDGEMENT

The authors are thankful to the Sophisticated Analytical Instrument Facility Laboratory (SAIF) at IIT Bombay for performing FT-IR, XRD, FEG-SEM and TEM-SAED measurements. The authors further extend their gratitude to Dr. Siddhivinayak Barve, KET's Scientific Research Centre (Mumbai)

for extending his support in conducting animal tissue culture studies.

## REFERENCES

- [1] K. A. Altammar. (2023). "A review on nanoparticles: characteristics, synthesis, applications, and challenges". *Frontiers in Microbiology*. **14** : 1155622. [10.3389/fmicb.2023.1155622](https://doi.org/10.3389/fmicb.2023.1155622).
- [2] R. Revathy, J. Joseph, C. Augustine, T. Sajini, and B. Mathew. (2022). "Synthesis and catalytic applications of silver nanoparticles: a sustainable chemical approach using indigenous reducing and capping agents from *Hyptis capitata*". *Environmental Science: Advances*. **1** (4): 491-505. [10.1039/d2va00044j](https://doi.org/10.1039/d2va00044j).
- [3] D. C. Lekha, R. Shanmugam, K. Madhuri, L. P. Dwarampudi, M. Bhaskaran, D. Kongara, J. L. Tesfaye, N. Nagaprasad, V. L. N. Bhargavi, R. Krishnaraj, and L. R. (2021). "Review on Silver Nanoparticle Synthesis Method, Antibacterial Activity, Drug Delivery Vehicles, and Toxicity Pathways: Recent Advances and Future Aspects". *Journal of Nanomaterials*. **2021** : 1-11. [10.1155/2021/4401829](https://doi.org/10.1155/2021/4401829).
- [4] L. Xu, Y. Y. Wang, J. Huang, C. Y. Chen, Z. X. Wang, and H. Xie. (2020). "Silver nanoparticles: Synthesis, medical applications and biosafety". *Theranostics*. **10** (20): 8996-9031. [10.7150/thno.45413](https://doi.org/10.7150/thno.45413).
- [5] N. Joudeh and D. Linke. (2022). "Nanoparticle classification, physicochemical properties, characterization, and applications: a comprehensive review for biologists". *Journal of Nanobiotechnology*. **20** (1): 262. [10.1186/s12951-022-01477-8](https://doi.org/10.1186/s12951-022-01477-8).
- [6] D. M. Metwally, R. A. Alajmi, M. F. El-Khadragy, and S. Al-Quraishy. (2020). "Silver Nanoparticles Biosynthesized With *Salvia officinalis* Leaf Exert Protective Effect on Hepatic Tissue Injury Induced by *Plasmodium chabaudi*". *Frontiers in Veterinary Science*. **7** : 620665. [10.3389/fvets.2020.620665](https://doi.org/10.3389/fvets.2020.620665).
- [7] H. I. O. Gomes, C. S. M. Martins, and J. A. V. Prior. (2021). "Silver Nanoparticles as Carriers of Anticancer Drugs for Efficient Target Treatment of Cancer Cells". *Nanomaterials (Basel)*. **11** (4). [10.3390/nano11040964](https://doi.org/10.3390/nano11040964).
- [8] R. Vishwanath and B. Negi. (2021). "Conventional and green methods of synthesis of silver nanoparticles and their antimicrobial properties". *Current Research in Green and Sustainable Chemistry*. **4**. [10.1016/j.crgsc.2021.100205](https://doi.org/10.1016/j.crgsc.2021.100205).
- [9] B. Venkataesan Kumari, R. Mani, B. R. Asokan, K. Balakrishnan, A. Ramasamy, R. Parthasarathi, C. Kandasamy, R. Govindaraj, N. Vijayakumar, and S. Vijayakumar. (2023). "Green Synthesised Silver Nanoparticles Using *Anoectochilus elatus* Leaf Extract: Characterisation and Evaluation of Antioxidant, Anti-Inflammatory, Antidiabetic, and Antimicrobial Activities". *Journal of Composites Science*. **7** (11). [10.3390/jcs7110453](https://doi.org/10.3390/jcs7110453).
- [10] Y. Li, Y. Jin, X. He, Y. Tang, M. Zhou, W. Guo, and W. Miao. (2022). "Cyclo(RGD) peptide-decorated silver nanoparticles with anti-platelet potential for active platelet-rich thrombus targeting". *Nanomedicine*. **41** : 102520. [10.1016/j.nano.2022.102520](https://doi.org/10.1016/j.nano.2022.102520).
- [11] P. Li, D. Karunanidhi, T. Subramani, and K. Srinivasamoorthy. (2021). "Sources and Consequences of Groundwater Contamination". *Archives of Environmental Contamination and Toxicology*. **80** (1): 1-10. [10.1007/s00244-020-00805-z](https://doi.org/10.1007/s00244-020-00805-z).
- [12] R. A. Kristanti, T. Hadibarata, M. Syafrudin, M. Yilmaz, and S. Abdullah. (2022). "Microbiological Contaminants in Drinking Water: Current Status and Challenges". *Water, Air, & Soil Pollution*. **233** (8). [10.1007/s11270-022-05698-3](https://doi.org/10.1007/s11270-022-05698-3).
- [13] P. K. Pandey, P. H. Kass, M. L. Soupir, S. Biswas, and V. P. Singh. (2014). "Contamination of water resources by pathogenic bacteria". *AMB Express*. **4** : 51. [10.1186/s13568-014-0051-x](https://doi.org/10.1186/s13568-014-0051-x).
- [14] N. V. Reddy, H. Li, T. Hou, M. S. Bethu, Z. Ren, and Z. Zhang. (2021). "Phytosynthesis of Silver Nanoparticles Using *Perilla frutescens* Leaf Extract: Characterization and Evaluation of Antibacterial, Antioxidant, and

- Anticancer Activities". *International Journal of Nanomedicine*. **16** : 15-29. [10.2147/IJN.S265003](https://doi.org/10.2147/IJN.S265003).
- [15] J. Kadam, P. Dhawal, S. Barve, and S. Kakodkar. (2020). "Green synthesis of silver nanoparticles using cauliflower waste and their multifaceted applications in photocatalytic degradation of methylene blue dye and Hg<sup>2+</sup> biosensing". *SN Applied Sciences*. **2** (4). [10.1007/s42452-020-2543-4](https://doi.org/10.1007/s42452-020-2543-4).
- [16] S. Iravani. (2014). "Bacteria in Nanoparticle Synthesis: Current Status and Future Prospects". *International Scholarly Research Notices*. **2014** : 359316. [10.1155/2014/359316](https://doi.org/10.1155/2014/359316).
- [17] C. Hano and B. H. Abbasi. (2021). "Plant-Based Green Synthesis of Nanoparticles: Production, Characterization and Applications". *Biomolecules*. **12** (1). [10.3390/biom12010031](https://doi.org/10.3390/biom12010031).
- [18] N. M. Alabdallah and M. M. Hasan. (2021). "Plant-based green synthesis of silver nanoparticles and its effective role in abiotic stress tolerance in crop plants". *Saudi Journal of Biological Sciences*. **28** (10): 5631-5639. [10.1016/j.sjbs.2021.05.081](https://doi.org/10.1016/j.sjbs.2021.05.081).
- [19] M. Pirsaeheb, T. Gholami, H. Seifi, E. A. Dawi, E. A. Said, A. M. Hamood, U. S. Altamari, and M. Salavati-Niasari. (2024). "Green synthesis of nanomaterials by using plant extracts as reducing and capping agents". *Environmental Science and Pollution Research*. **31** (17): 24768-24787. [10.1007/s11356-024-32983-x](https://doi.org/10.1007/s11356-024-32983-x).
- [20] C. Vanlalveni, S. Lallianrawna, A. Biswas, M. Selvaraj, B. Changmai, and S. L. Rokhum. (2021). "Green synthesis of silver nanoparticles using plant extracts and their antimicrobial activities: a review of recent literature". *RSC Advances*. **11** (5): 2804-2837. [10.1039/d0ra09941d](https://doi.org/10.1039/d0ra09941d).
- [21] M. S. Waghmode, A. B. Gunjal, N. N. Nawani, and N. N. Patil. (2016). "Management of Floral Waste by Conversion to Value-Added Products and Their Other Applications". *Waste and Biomass Valorization*. **9** (1): 33-43. [10.1007/s12649-016-9763-2](https://doi.org/10.1007/s12649-016-9763-2).
- [22] A. L. Srivastav and A. Kumar. (2021). "An endeavor to achieve sustainable development goals through floral waste management: A short review". *Journal of Cleaner Production*. **283**. [10.1016/j.jclepro.2020.124669](https://doi.org/10.1016/j.jclepro.2020.124669).
- [23] A. Nair, A. Kelkar, S. Kshirsagar, A. Harekar, K. Satardekar, S. Barve, and S. Kakodkar. (2018). "Extraction of natural dye from waste flowers of Aster (*Aster chinensis*) and studying its potential application as pH indicator". *Journal of Innovations in Pharmaceutical and Biological Sciences*. **5** : 1-4.
- [24] S. A. Kakodkar, S. N. Kshirsagar, A. S. Kelkar, A. M. Nair, P. P. Dhawal, K. V. Satardekar, and S. S. Barve. (2019). "Evaluation of phytochemical constituents, antioxidant property, DNA damage inhibition activity and cytotoxicity of aster (*Callistephus chinensis*) flower waste". *World Journal of Pharmaceutical Research*. **8** : 977-991.
- [25] I. Ashraf, A. Agarwal, N. B. Singh, and M. B. Ray. (2023). "Floral waste synthesized silver nanoparticles as sensor for Cr (VI) ion detection". *Environmental Monitoring and Assessment*. **195** (6): 671. [10.1007/s10661-023-11342-2](https://doi.org/10.1007/s10661-023-11342-2).
- [26] J. B. Johnson, J. S. Mani, and M. Naiker. (2023). "Microplate Methods for Measuring Phenolic Content and Antioxidant Capacity in Chickpea: Impact of Shaking". *Engineering Proceedings*. **48** (1): 57. [10.3390/CSAC2023-15167](https://doi.org/10.3390/CSAC2023-15167).
- [27] A. Fatiqin, H. Amrulloh, W. Simanjuntak, I. Apriani, R. A. H. T. Amelia, S. Syarifah, R. N. Sunarti, and A. R. P. Raharjeng. (2021). "Characteristics of nano-size MgO prepared using aqueous extract of different parts of *Moringa oleifera* plant as green synthesis agents". *AIP Conference Proceedings*. [10.1063/5.0041999](https://doi.org/10.1063/5.0041999).
- [28] N. A. Rahim, M. N. F. Roslan, M. Muhamad, and A. Seenii. (2022). "Antioxidant Activity, Total Phenolic and Flavonoid Content and LC-MS Profiling of Leaves Extracts of *Alstonia angustiloba*". *Separations*. **9** (9). [10.3390/separations9090234](https://doi.org/10.3390/separations9090234).

- [29] N. Sanchooli, S. Saeidi, H. K. Barani, and E. Sanchooli. (2018). "In vitro antibacterial effects of silver nanoparticles synthesized using *Verbena officinalis* leaf extract on *Yersinia ruckeri*, *Vibrio cholera* and *Listeria monocytogenes*". *Iranian Journal of Microbiology*. **10** : 400-408.
- [30] F. Mallevre, C. Alba, C. Milne, S. Gillespie, T. F. Fernandes, and T. J. Aspray. (2016). "Toxicity Testing of Pristine and Aged Silver Nanoparticles in Real Wastewaters Using Bioluminescent *Pseudomonas putida*". *Nanomaterials (Basel)*. **6** (3). [10.3390/nano6030049](https://doi.org/10.3390/nano6030049).
- [31] A. O. Edegbene, D. Yandev, T. O. Omotehinwa, H. Zakari, and B. O. Andy. (2025). "Water quality assessment in Benue South, Nigeria: An investigation of physico-chemical and microbial characteristics". *Water Science*. **39** (1): 279-290. [10.1080/23570008.2025.2483013](https://doi.org/10.1080/23570008.2025.2483013).
- [32] P. J. Utgikar, J. H. Kadam, S. J. Rambhiya, V. M. Inamdar, P. D. Nagda, S. S. Barve, and P. P. Dhawal. (2022). "Titanium Dioxide and Its Effect on Human Health and Environment - An in vitro Study". *European Journal of Biology and Biotechnology*. **3** (2): 20-24. [10.24018/ejbio.2022.3.2.352](https://doi.org/10.24018/ejbio.2022.3.2.352).
- [33] V. Vichai and K. Kirtikara. (2006). "Sulforhodamine B colorimetric assay for cytotoxicity screening". *Nature Protocols*. **1** (3): 1112-6. [10.1038/nprot.2006.179](https://doi.org/10.1038/nprot.2006.179).
- [34] F. Rodriguez-Felix, A. G. Lopez-Cota, M. J. Moreno-Vasquez, A. Z. Graciano-Verdugo, I. E. Quintero-Reyes, C. L. Del-Toro-Sanchez, and J. A. Tapia-Hernandez. (2021). "Sustainable-green synthesis of silver nanoparticles using safflower (*Carthamus tinctorius* L.) waste extract and its antibacterial activity". *Heliyon*. **7** (4): e06923. [10.1016/j.heliyon.2021.e06923](https://doi.org/10.1016/j.heliyon.2021.e06923).
- [35] F. Zia, N. Ghafoor, M. Iqbal, and S. Mehboob. (2016). "Green synthesis and characterization of silver nanoparticles using *Cydonia oblong* seed extract". *Applied Nanoscience*. **6** (7): 1023-1029. [10.1007/s13204-016-0517-z](https://doi.org/10.1007/s13204-016-0517-z).
- [36] Y. He, Z. Du, H. Lv, Q. Jia, Z. Tang, X. Zheng, K. Zhang, and F. Zhao. (2013). "Green synthesis of silver nanoparticles by *Chrysanthemum morifolium* Ramat. extract and their application in clinical ultrasound gel". *International Journal of Nanomedicine*. **8** : 1809-15. [10.2147/IJN.S43289](https://doi.org/10.2147/IJN.S43289).
- [37] S. Devanesan and M. S. AlSalhi. (2021). "Green Synthesis of Silver Nanoparticles Using the Flower Extract of *Abelmoschus esculentus* for Cytotoxicity and Antimicrobial Studies". *International Journal of Nanomedicine*. **16** : 3343-3356. [10.2147/IJN.S307676](https://doi.org/10.2147/IJN.S307676).
- [38] O. Sabira, A. P. Ajaykumar, S. R. Varma, K. N. Jayaraj, M. Kotakonda, P. Kumar, P. Vaikkathillam, V. Sivadasan Binitha, A. P. Alen, A. V. Raghu, and K. V. Zeena. (2025). "Nepenthes pitcher fluid for the green synthesis of silver nanoparticles with biofilm inhibition, anticancer and antioxidant properties". *Scientific Reports*. **15** (1): 5349. [10.1038/s41598-025-89212-9](https://doi.org/10.1038/s41598-025-89212-9).
- [39] A. Wirwis and Z. Sadowski. (2023). "Green Synthesis of Silver Nanoparticles: Optimizing Green Tea Leaf Extraction for Enhanced Physicochemical Properties". *ACS Omega*. **8** (33): 30532-30549. [10.1021/acsomega.3c03775](https://doi.org/10.1021/acsomega.3c03775).
- [40] A. S. Folorunso. (2019). "Characterization And Antimicrobial Investigation Of Synthesized Silver Nanoparticles From *Annona Muricata* Leaf Extracts". *Nanotechnology Nanomedicine & Nanobiotechnology*. **6** (1): 1-5. [10.24966/ntmb-2044/100022](https://doi.org/10.24966/ntmb-2044/100022).
- [41] J. Santhoshkumar, S. Rajeshkumar, and S. Venkat Kumar. (2017). "Phyto-assisted synthesis, characterization and applications of gold nanoparticles - A review". *Biochemistry and Biophysics Reports*. **11** : 46-57. [10.1016/j.bbrep.2017.06.004](https://doi.org/10.1016/j.bbrep.2017.06.004).
- [42] O. Velgosova, S. Dolinska, H. Podolska, L. Macak, and E. Cizmarova. (2024). "Impact of Plant Extract Phytochemicals on the Synthesis of Silver Nanoparticles". *Materials (Basel)*. **17** (10). [10.3390/ma17102252](https://doi.org/10.3390/ma17102252).
- [43] P. Devaraj, P. Kumari, C. Aarti, and A. Renganathan. (2013). "Synthesis and Characterization of Silver Nanoparticles Using Cannonball Leaves and Their



- Cytotoxic Activity against MCF-7 Cell Line". *Journal of Nanotechnology*. **2013** : 1-5. [10.1155/2013/598328](https://doi.org/10.1155/2013/598328).
- [44] K. Roy, C. K. Sarkar, and C. K. Ghosh. (2014). "Photocatalytic activity of biogenic silver nanoparticles synthesized using yeast (*Saccharomyces cerevisiae*) extract". *Applied Nanoscience*. **5** (8): 953-959. [10.1007/s13204-014-0392-4](https://doi.org/10.1007/s13204-014-0392-4).
- [45] S. Jain and M. S. Mehata. (2017). "Medicinal Plant Leaf Extract and Pure Flavonoid Mediated Green Synthesis of Silver Nanoparticles and their Enhanced Antibacterial Property". *Scientific Reports*. **7** (1): 15867. [10.1038/s41598-017-15724-8](https://doi.org/10.1038/s41598-017-15724-8).
- [46] M. Bhusal, I. Pathak, A. Bhadel, D. K. Shrestha, and K. R. Sharma. (2024). "Synthesis of silver nanoparticles assisted by aqueous root and leaf extracts of *Rhus chinensis* Mill and its antibacterial activity". *Heliyon*. **10** (13): e33603. [10.1016/j.heliyon.2024.e33603](https://doi.org/10.1016/j.heliyon.2024.e33603).
- [47] F. Lalsangpuui, S. L. Rokhum, F. Nghakliana, L. Fakawmi, J. V. L. Ruatpuia, E. Laltlanmawii, R. Lalfakzuala, and Z. Siama. (2022). "Green Synthesis of Silver Nanoparticles Using *Spilanthes acmella* Leaf Extract and its Antioxidant-Mediated Ameliorative Activity against Doxorubicin-Induced Toxicity in Dalton's Lymphoma Ascites (DLA)-Bearing Mice". *ACS Omega*. **7** (48): 44346-44359. [10.1021/acsomega.2c05970](https://doi.org/10.1021/acsomega.2c05970).
- [48] K. Okaiyeto, M. O. Ojemaye, H. Hoppe, L. V. Mabinya, and A. I. Okoh. (2019). "Phytofabrication of Silver/Silver Chloride Nanoparticles Using Aqueous Leaf Extract of *Oedera genistifolia*: Characterization and Antibacterial Potential". *Molecules*. **24** (23). [10.3390/molecules24234382](https://doi.org/10.3390/molecules24234382).
- [49] B. R. Jany, A. Janas, and F. Krok. (2017). "Retrieving the Quantitative Chemical Information at Nanoscale from Scanning Electron Microscope Energy Dispersive X-ray Measurements by Machine Learning". *Nano Letters*. **17** (11): 6520-6525. [10.1021/acs.nanolett.7b01789](https://doi.org/10.1021/acs.nanolett.7b01789).
- [50] N. S. Swidan, Y. A. Hashem, W. F. Elkhatab, and M. A. Yassien. (2022). "Antibiofilm activity of green synthesized silver nanoparticles against biofilm associated enterococcal urinary pathogens". *Scientific Reports*. **12** (1): 3869. [10.1038/s41598-022-07831-y](https://doi.org/10.1038/s41598-022-07831-y).
- [51] I. A. M. Ali, A. B. Ahmed, and H. I. Al-Ahmed. (2023). "Green synthesis and characterization of silver nanoparticles for reducing the damage to sperm parameters in diabetic compared to metformin". *Scientific Reports*. **13** (1): 2256. [10.1038/s41598-023-29412-3](https://doi.org/10.1038/s41598-023-29412-3).
- [52] A. Abbaszadegan, Y. Ghahramani, A. Gholami, B. Hemmateenejad, S. Dorostkar, M. Nabavizadeh, H. Sharghi, and R. Hazan. (2015). "The Effect of Charge at the Surface of Silver Nanoparticles on Antimicrobial Activity against Gram-Positive and Gram-Negative Bacteria: A Preliminary Study". *Journal of Nanomaterials*. **2015** (1). [10.1155/2015/720654](https://doi.org/10.1155/2015/720654).
- [53] M. Ozdal and S. Gurkok. (2022). "Recent advances in nanoparticles as antibacterial agent". *ADMET and DMPK*. **10** (2): 115-129. [10.5599/admet.1172](https://doi.org/10.5599/admet.1172).
- [54] S. Shaikh, N. Nazam, S. M. D. Rizvi, K. Ahmad, M. H. Baig, E. J. Lee, and I. Choi. (2019). "Mechanistic Insights into the Antimicrobial Actions of Metallic Nanoparticles and Their Implications for Multidrug Resistance". *International Journal of Molecular Sciences*. **20** (10). [10.3390/ijms20102468](https://doi.org/10.3390/ijms20102468).
- [55] M. Singh, S. Singh, S. Prasad, and I. Gambhir. (2008). "Nanotechnology in medicine and antibacterial effect of silver nanoparticles". *Digest Journal of Nanomaterials and Biostructures*. **3** (3): 115-122.
- [56] P. R. More, S. Pandit, A. Filippis, G. Franci, I. Mijakovic, and M. Galdiero. (2023). "Silver Nanoparticles: Bactericidal and Mechanistic Approach against Drug Resistant Pathogens". *Microorganisms*. **11** (2). [10.3390/microorganisms11020369](https://doi.org/10.3390/microorganisms11020369).
- [57] N. Paracini, E. Schneck, A. Imberty, and S. Micciulla. (2022). "Lipopolysaccharides at Solid and Liquid Interfaces: Models for Biophysical Studies of the Gram-negative

- Bacterial Outer Membrane". *Advances in Colloid and Interface Science*. **301** : 102603. [10.1016/j.cis.2022.102603](https://doi.org/10.1016/j.cis.2022.102603).
- [58] E. O. Mikhailova. (2020). "Silver Nanoparticles: Mechanism of Action and Probable Bio-Application". *Journal of Functional Biomaterials*. **11** (4). [10.3390/jfb11040084](https://doi.org/10.3390/jfb11040084).
- [59] R. R. Krishnan, K. Dharmaraj, and B. D. R. Kumari. (2007). "A comparative study on the physicochemical and bacterial analysis of drinking, borewell and sewage water in the three different places of Sivakasi". *Journal of Environmental Biology*. **28** : 105-108.
- [60] S. Some, R. Mondal, D. Mitra, D. Jain, D. Verma, and S. Das. (2021). "Microbial pollution of water with special reference to coliform bacteria and their nexus with environment". *Energy Nexus*. **1**. [10.1016/j.nexus.2021.100008](https://doi.org/10.1016/j.nexus.2021.100008).
- [61] M. Morais, A. L. Teixeira, F. Dias, V. Machado, R. Medeiros, and J. A. V. Prior. (2020). "Cytotoxic Effect of Silver Nanoparticles Synthesized by Green Methods in Cancer". *Journal of Medicinal Chemistry*. **63** (23): 14308-14335. [10.1021/acs.jmedchem.0c01055](https://doi.org/10.1021/acs.jmedchem.0c01055).
- [62] H. S. Hussein, C. Ngugi, F. M. Tolo, and E. N. Maina. (2024). "Anticancer potential of silver nanoparticles biosynthesized using Catharanthus roseus leaves extract on cervical (HeLa229) cancer cell line". *Scientific African*. **25**. [10.1016/j.sciaf.2024.e02268](https://doi.org/10.1016/j.sciaf.2024.e02268).
- [63] X. Liu, K. Shan, X. Shao, X. Shi, Y. He, Z. Liu, J. A. Jacob, and L. Deng. (2021). "Nanotoxic Effects of Silver Nanoparticles on Normal HEK-293 Cells in Comparison to Cancerous HeLa Cell Line". *International Journal of Nanomedicine*. **16** : 753-761. [10.2147/IJN.S289008](https://doi.org/10.2147/IJN.S289008).
- [64] R. Sukirtha, K. M. Priyanka, J. J. Antony, S. Kamalakkannan, R. Thangam, P. Gunasekaran, M. Krishnan, and S. Achiraman. (2012). "Cytotoxic effect of Green synthesized silver nanoparticles using Melia azedarach against in vitro HeLa cell lines and lymphoma mice model". *Process Biochemistry*. **47** (2): 273-279. [10.1016/j.procbio.2011.11.003](https://doi.org/10.1016/j.procbio.2011.11.003).